

Boundary and finite-size effects in small magnetic systems

H Kachkachi* and D A Garanin[†]

*Laboratoire de Magnétisme et d'Optique, Université de Versailles St. Quentin, 45 av. des Etats-Unis, 78035 Versailles, France

[†]Max-Planck-Institut für Physik komplexer Systeme, Nöthnitzer Strasse 38, D-01187 Dresden, Germany

Received 19 January 2000

Abstract. We study the effect of free boundaries in finite magnetic systems of cubic shape on the field and temperature dependence of the magnetization within the isotropic model of D -component spin vectors in the limit $D \rightarrow \infty$. This model is described by a closed system of equations and captures the Goldstone-mode effects such as global rotation of the magnetic moment and spin-wave fluctuations. We have obtained an exact relation between the intrinsic (short-range) magnetization $M = M(H, T)$ of the system and the supermagnetization $m = m(H, T)$ which is induced by the field. We have shown, analytically at low temperatures and fields and numerically in a wide range of these parameters, that boundary effects leading to the decrease of M with respect to the bulk value are stronger than the finite-size effects making a positive contribution to M . The inhomogeneities of the magnetization caused by the boundaries are long ranged and extend far into the depth of the system.

1 Introduction

Small magnetic particles have been of much interest owing to their technological applications, mainly in the area of information storage. From the experimental and theoretical point of view, these systems are very interesting for they show superparamagnetism and exponentially slow relaxation rates at low temperatures due to anisotropy barriers. Although in the most of theoretical approaches to the dynamics of a small magnetic particle the latter is considered as a single magnetic moment, deviations from this simple picture become crucial with the reduction of the system size. In magnetic *nanoparticles* (see, for a review, Ref. [1]), the contribution of the surface to the thermodynamic properties becomes comparable with the bulk contribution, and the magnetization and other characteristics may be spatially inhomogeneous. The latter is realized due to additional thermal disordering near the surface at elevated temperatures or due to the breaking of symmetry of the crystal field for surface spins, which may result in a strong surface anisotropy. Another manifestation of the symmetry breaking at the surface is the possible unquenching of the orbital moments of surface spins, which may be responsible for a significant increase of the particle's magnetic moment, e.g. in $3d$ elements [2].

*kachkach@physique.uvsq.fr

[†]www.mpi-pks-dresden.mpg.de/~garanin/; garanin@mpi-pks-dresden.mpg.de

A finite-size magnetic system with realistic free boundary conditions presents a spatially inhomogeneous many-body problem. A great deal of work up to date has been based on the Monte Carlo (MC) technique for the Ising model. MC technique was also used with the more adequate classical Heisenberg model to simulate idealized isotropic nanoparticles with simple cubic (sc) structure and spherical shape in Ref. [3]. Magnetic nanoparticles with realistic lattice structure were simulated, e.g., in Ref. [4] taking into account surface anisotropy and dipole-dipole interaction.

Familiar analytical methods such as the mean-field approximation (MFA) and spin-wave theory (SWT) are inappropriate for finite magnetic systems because of the Goldstone mode corresponding to the global rotation of the magnetic moments in zero field. A more sophisticated way to analytically treat finite magnets is to take the limit $D \rightarrow \infty$ for the model of D -component classical spin vectors, which was introduced by Stanley [5]. Stanley has shown [6] that for $D \rightarrow \infty$ the partition function for this model in the bulk coincides with that of the exactly solvable spherical model (SM) [7]. Both models provide a reasonably good approximation (about 5% overall accuracy) to the isotropic classical Heisenberg model in three dimensions. For spatially inhomogeneous systems such as magnetic particles or films with free boundary conditions (fbc), these two models become nonequivalent, the SM having been shown to yield unphysical results because of the inappropriate global spin constraint [8]. This drawback was fixed in an improved version of the SM using *local* spin constraints on each lattice site [9, 10]. Yet two profound differences between the $D \rightarrow \infty$ model and the SM cannot be eliminated. First, there are two (longitudinal and transverse) correlation functions in the former [11] and only one CF in the latter. Second, generalization for the anisotropic case is only possible for the $D \rightarrow \infty$ model. The resulting anisotropic spherical model (ASM) was applied to describe phase transitions in domain walls [12] and in magnetic films [13]. The main feature of the $D \rightarrow \infty$ model or the ASM is that it takes into account Goldstone modes in the system, which prevent phase transitions for isotropic systems in dimensions $d \leq 2$. In contrast with the linear SWT, this model self-consistently generates a gap in the correlation functions which avoids the infrared divergencies. Anisotropy plays a crucial role in these systems since it breaks the symmetry of the system and makes phase transitions in two dimensions possible.

So far, the ASM was only applied to spatially inhomogeneous systems in the plane geometry [12, 13, 14]. Here we extend it for *finite* magnetic systems in the box geometry with free and periodic boundary conditions (fbc and pbc), restricting ourselves to the idealized case of isotropic coupling and simple cubic lattice and reserving consideration of realistic lattice structures, bulk and surface anisotropies, etc., for the subsequent work. We obtain analytical asymptotes at low temperatures and fields and a complete numerical solution in the whole range of T and H for the intrinsic magnetization $M = M(H, T)$ and the supermagnetization $m = m(H, T)$, and we prove the *exact* relation $m = MB(\mathcal{N}MH/T)$ between them, $\mathcal{N} = N_x N_y N_z$ being the number of sites in the system and $B(x)$ being the Langevin function. For the system with fbc, the value of M is significantly reduced with respect to that for the pbc model and to the bulk due to the boundary effects. We consider temperature dependences of *local* magnetization M_i and estimate the critical indices for the magnetization at the faces, edges, and corners of the system. We show that because of the Goldstone modes, the inhomogeneities of M_i extend far into the depth of the particle, i.e., the magnetization profile in our isotropic model is long ranged. This feature is in accord with the MC simulations for the Heisenberg model [3, 4], as opposed to the MFA predictions [3].

The rest of the paper is organized as follows. In Sec. 2 we write down the equations describing the spatially inhomogeneous ASM *in a magnetic field*, generalizing the results of Ref. [12]. Further, restricting ourselves to the isotropic model, we define the magnetizations mentioned above and derive relations between them. In Sec. 3

we consider the model with periodic boundary conditions and derive low-temperature and low-field analytical expressions for the intrinsic magnetization. In Sec. 4 we take into account boundary effects for the fbc model at low temperatures. In Sec. 5 the numerical results for the temperature, field, and spatial dependencies of the magnetization of finite magnetic systems are presented.

2 Hamiltonian and basic equations

We start with the Hamiltonian of the uniaxially anisotropic classical D -component vector model, which can be written in the form

$$\mathcal{H} = -\mathbf{H} \cdot \sum_i \mathbf{s}_i - \frac{1}{2} \sum_{i,j} J_{ij} \left(s_{zi} s_{zj} + \eta \sum_{\alpha=2}^D s_{\alpha i} s_{\alpha j} \right), \quad (2.1)$$

where \mathbf{s}_i is the normalized D -component vector, $|\mathbf{s}_i| = 1$, and $\eta \leq 1$ is the dimensionless anisotropy factor; \mathbf{H} is the magnetic field, and J_{ij} the exchange coupling.

In the mean-field approximation the Curie temperature of this model is $T_c^{\text{MFA}} = J_0/D$, where J_0 is the zero Fourier component of J_{ij} . It is convenient to use T_c^{MFA} as the energy scale and introduce the dimensionless variables

$$\theta \equiv T/T_c^{\text{MFA}}, \quad \mathbf{h} \equiv \mathbf{H}/J_0, \quad \lambda_{ij} \equiv J_{ij}/J_0. \quad (2.2)$$

For the nearest-neighbour (nn) interaction J_{ij} with z neighbours, λ_{ij} is equal to $1/z$ if sites i and j are nearest neighbours and zero otherwise.

Using the diagram technique for classical spin systems [15, 16, 17] in the limit $D \rightarrow \infty$ and generalizing the results of Ref. [12] for spatially inhomogeneous systems to include the magnetic field $\mathbf{h} = h_x \mathbf{e}_x + h_z \mathbf{e}_z$, one arrives at the closed system of equations for the average magnetization components $\alpha = 1$ (z) and $\alpha = 2$ (x) and correlation functions for remaining spin components labelled by $\alpha \geq 3$,

$$m_{xi} \equiv \langle s_{xi} \rangle, \quad m_{zi} \equiv \langle s_{zi} \rangle, \quad s_{ij} \equiv D \langle s_{\alpha i} s_{\alpha j} \rangle. \quad (2.3)$$

Here all correlation functions are equal to each other by symmetry. The system of equations describing the anisotropic spherical model consists of equations for the magnetization components

$$m_{xi} = G_i(h_x + \eta \sum_j \lambda_{ij} m_{xj}), \quad m_{zi} = G_i(h_z + \sum_j \lambda_{ij} m_{zj}), \quad (2.4)$$

and the Dyson equation for the correlation function

$$s_{il} = \theta G_i \delta_{il} + \eta G_i \sum_j \lambda_{ij} s_{jl}, \quad (2.5)$$

where δ_{il} is the Kronecker symbol. G_i is the so-called *gap parameter* to be determined from the set of constraint equations on all sites $i = 1, \dots, \mathcal{N}$ of the lattice

$$s_{ii} + \mathbf{m}_i^2 = 1, \quad (2.6)$$

where $\mathbf{m}_i^2 = m_{zi}^2 + m_{xi}^2$.

The system of equations above describing the anisotropic spherical model (ASM) will be used in its full form elsewhere. In the present work, we will consider isotropic ($\eta = 1$) magnetic systems of box shape of volume $\mathcal{N} = N_x N_y N_z$, with simple-cubic lattice structure, and nearest-neighbour exchange coupling, in a uniform magnetic field. In this model, the magnetization \mathbf{m} is directed along the field \mathbf{h} , thus one

can set $\mathbf{h} = h\mathbf{e}_z$ and $\mathbf{m}_i = m_i\mathbf{e}_z$. In the limit of $D \rightarrow \infty$ it becomes immaterial what is the exact number of “transverse” components: $D - 2$ for the anisotropic model, Eq. (2.3), $D - 1$ for the isotropic model in field (the case we are considering here), or D for the isotropic model in zero field. In general, there are a few components with nonvanishing averages $\langle s_\alpha \rangle$, and the remaining components called “transverse” components, are booked into the correlation functions.

Solving the system of equations above consists in determining \mathbf{m}_i and s_{ij} as functions of G_i from the linear equations (2.4) and (2.5), respectively, and inserting these solutions in the constraint equation (2.6) in order to obtain G_i . The two main types of boundary conditions for our problem are free boundary conditions (fbc) and periodic boundary conditions (pbc). In the case of fbc, if the summation index j in Eqs. (2.4) and (2.5) runs out of the lattice, the corresponding terms are omitted. In this case, \mathbf{m}_i and G_i are inhomogeneous and s_{ij} nontrivially depends on both indices due to boundary effects. In the pbc case the solution becomes homogeneous and greatly simplifies. Although the model with pbc is unphysical, it allows for an analytical treatment at all temperatures and for the study of finite-size effects separately from boundary effects.

One can also introduce a matrix formalism and rewrite Eqs. (2.4) and (2.5) for the isotropic model in field as follows

$$\sum_j \mathcal{D}_{ij} m_j = h, \quad \sum_j \mathcal{D}_{ij} s_{jl} = \theta \delta_{il}, \quad (2.7)$$

where we have defined the Dyson matrix $\mathcal{D}_{ij} \equiv G_i^{-1} \delta_{ij} - \lambda_{ij}$. The solutions of these linear equations are

$$m_i = h \sum_j \mathcal{D}_{ij}^{-1}, \quad s_{ij} = \theta \mathcal{D}_{ij}^{-1}, \quad (2.8)$$

\mathcal{D}^{-1} being the inverse of the Dyson matrix \mathcal{D} . Substituting these solutions into the constraint equation (2.6) results in a closed system of nonlinear equations for the gap parameter G_i

$$\left(h \sum_j \mathcal{D}_{ij}^{-1} \right)^2 + \theta \mathcal{D}_{ii}^{-1} = 1. \quad (2.9)$$

The average magnetization per site defined by

$$\mathbf{m} = \frac{1}{\mathcal{N}} \sum_i \mathbf{m}_i \quad (2.10)$$

vanishes for finite-size systems in the absence of magnetic field due to the Goldstone mode corresponding to the global rotation of the magnetization. On the other hand, it is clear that at temperatures $\theta \ll 1$ the spins in the system are aligned with respect to each other and there should exist an *intrinsic* magnetization. The latter is usually defined for finite-size systems as

$$M = \sqrt{\left\langle \left(\frac{1}{\mathcal{N}} \sum_i \mathbf{s}_i \right)^2 \right\rangle} = \sqrt{\mathbf{m}^2 + \frac{1}{\mathcal{N}^2} \sum_{i,j=1}^{\mathcal{N}} s_{ij}}, \quad (2.11)$$

where the second expression is valid in the limit $D \rightarrow \infty$. Here \mathbf{m} and s_{ij} are defined by Eqs. (2.3) and (2.10). One can see that $M \geq m$. Note that M remains non zero for $h = 0$. In this case in the limit $\theta \rightarrow 0$ one has $s_{ij} = 1$ for all i and j , and $M \rightarrow 1$. For $\theta \rightarrow \infty$ the spins becomes uncorrelated, $s_{ij} = \delta_{ij}$, and $M \rightarrow 1/\sqrt{\mathcal{N}}$. In the limit of $\mathcal{N} \rightarrow \infty$, the intrinsic magnetization M approaches that of the bulk system.

The applied field suppresses the global-rotation Goldstone mode and thereby renders the magnetization \mathbf{m} of Eq.(2.10) non zero. Therefore, it is convenient to call the latter the *supermagnetization*, in contrast with the intrinsic magnetization M . If the field is strong or the temperature is low, the spins align along the field, the transverse correlation functions s_{ij} in Eq. (2.11) become small, and the magnitude of the supermagnetization approaches the intrinsic magnetization.

One can establish an important relation between the intrinsic magnetization M and supermagnetization m . To this end, one first obtains from Eqs. (2.8) and (2.10) the useful relation

$$\frac{1}{\mathcal{N}^2} \sum_{ij} s_{ij} = \frac{\theta}{\mathcal{N}} \frac{m}{h}. \quad (2.12)$$

Then, substituting the latter in Eq. (2.11) and solving the equation thus obtained, $m^2 + \theta m/(\mathcal{N}h) - M^2 = 0$, for m yields

$$m = M \frac{2\mathcal{N}Mh/\theta}{1 + \sqrt{1 + (2\mathcal{N}Mh/\theta)^2}} = MB(\mathcal{N}MH/T), \quad (2.13)$$

where $B(\xi) = (2\xi/D)/[1 + \sqrt{1 + (2\xi/D)^2}]$ is the Langevin function for $D \gg 1$. One can find in the literature formulae of the type $m = M_s B(\mathcal{N}M_s H/T)$, where M_s are *ad hoc* quantities with slightly different meanings. In our case, Eq. (2.13) is exact and $M = M(T, H)$ is explicitly defined by Eq. (2.11). For large sizes \mathcal{N} , Eq. (2.13) describes two distinct field ranges separated at $h \sim h^*$ where

$$h^* \equiv \frac{\theta}{\mathcal{N}M_0(\theta)}, \quad M_0(\theta) \equiv M(\theta, h = 0). \quad (2.14)$$

In the range $h \lesssim h^*$, the total magnetic moment of the system is disoriented by thermal fluctuations, and the supermagnetization m is essentially lower than the intrinsic magnetization M . In the range $h \gtrsim h^*$, the total magnetic moment is oriented by the field, m approaches M , and both the latter further increase with field towards saturation ($m = M = 1$) due to the suppression of spin waves in the system. This scenario is quite general and inherent to all $O(D)$ models, as was shown on phenomenological grounds in Ref. [18]. Early Monte Carlo simulations of Ref. [3] for isotropic Heisenberg systems of spherical shape confirm Eq. (2.13) within statistical errors, although the accuracy is not high enough to decide whether this relation is exact.

One can also consider local magnetizations. The local supermagnetization is simply the vector \mathbf{m}_i , while the local intrinsic magnetization can be defined as follows

$$M_i = \frac{1}{M} \left\langle \mathbf{s}_i \cdot \frac{1}{\mathcal{N}} \sum_j \mathbf{s}_j \right\rangle = \frac{1}{\mathcal{N}M} \sum_{j=1}^{\mathcal{N}} (s_{ij} + \mathbf{m}_i \cdot \mathbf{m}_j) \quad (2.15)$$

One can check the identity $(1/\mathcal{N}) \sum_i M_i = M$ showing the self-consistency of the definition given above.

We start by considering the pbc model in the next section.

3 Systems with periodic boundary conditions

In this case, as was said above, the system becomes homogeneous, that is $G_i = G$, $\mathbf{m}_i = \mathbf{m}$, and the correlation functions can be found by performing a Fourier transformation of the type

$$F_i = \frac{1}{\mathcal{N}} \sum_{\mathbf{k}} e^{-i\mathbf{k}\mathbf{r}_i} F_{\mathbf{k}}, \quad F_{\mathbf{k}} = \sum_i e^{i\mathbf{k}\mathbf{r}_i} F_i, \quad (3.16)$$

where for a cube $\mathcal{N} = N^3$ one has

$$k_\alpha = 2\pi n_\alpha/N, \quad n_\alpha = 0, 1, \dots, N-1, \quad \alpha = x, y, z. \quad (3.17)$$

This results in

$$s_{ii} = \frac{1}{\mathcal{N}} \sum_{\mathbf{k}} s_{\mathbf{k}} = \theta GP_N(G), \quad (3.18)$$

where

$$P_N(G) = \frac{1}{\mathcal{N}(1-G)} + \tilde{P}_N(G), \quad \tilde{P}_N(G) \equiv \frac{1}{\mathcal{N}} \sum'_{\mathbf{k}} \frac{1}{1-G\lambda_{\mathbf{k}}} \quad (3.19)$$

and $\lambda_{\mathbf{k}} = J_{\mathbf{k}}/J_0$. In the lattice Green function $\overline{P}_N(G)$ the contributions of the would-be Goldstone mode with $\mathbf{k} = \mathbf{0}$ and other modes have been separated from each other. In the bulk limit $N \rightarrow \infty$ for the sc lattice

$$P_\infty(G) \equiv P(G) \cong \begin{cases} 1 + G^2/(2d), & G \ll 1 \\ W - c_0\sqrt{1-G}, & 1-G \ll 1, \end{cases} \quad (3.20)$$

where $d = 3$, the Watson integral $W = 1.51639$, and $c_0 = (2/\pi)(3/2)^{3/2}$. The difference between the sum and the integral,

$$W_N^{(\text{pbc})} = \frac{1}{\mathcal{N}} \sum'_{\mathbf{k}} \frac{1}{1-\lambda_{\mathbf{k}}} \quad \text{and} \quad W = \int \frac{d^3\mathbf{k}}{(2\pi)^3} \frac{1}{1-\lambda_{\mathbf{k}}}, \quad (3.21)$$

describes the finite-size effect and for the sc lattice, $\lambda_{\mathbf{k}} = (\cos k_x + \cos k_y + \cos k_z)/3$, behaves as $1/N$ [19]

$$\Delta_N^{(\text{pbc})} \equiv \frac{W_N^{(\text{pbc})} - W}{W} \cong -\frac{0.90}{N}, \quad N \gg 1. \quad (3.22)$$

The easiest way to obtain the coefficient in this formula is to plot $\Delta_N^{(\text{pbc})}$ vs $1/N$ (see Fig. 1). For finite N , $\tilde{P}_N(G)$ becomes regular at $G = 1$. In the large- N limit for $1-G \ll k_{\min}^2 \sim 1/N^2$, where $k_{\min} \sim 1/N$ is the minimal wave vector in a finite-size system, one has

$$\tilde{P}_N(G) \cong W_N^{(\text{pbc})} - cN(1-G), \quad c = \sum'_{n_x, n_y, n_z = -\infty}^{\infty} \frac{36}{(n_x^2 + n_y^2 + n_z^2)^2} \simeq 596. \quad (3.23)$$

For larger $1-G$, the square-root singularity Eq. (3.20) is restored.

Using $\sum_j \lambda_{ij} = 1$ in the second of Eqs. (2.4), one arrives in the isotropic case $\eta = 1$, at the system of equations

$$m = \frac{hG}{1-G}, \quad m^2 + \theta GP_N(G) = 1. \quad (3.24)$$

The solution $G(\theta)$ of these equations decreases with increasing temperature, and at high temperatures, the leading asymptote is $G = 1/\theta$. For the bulk system at low temperatures or high fields, G tends to $1/(1+h)$. For finite-size systems, even in zero field, the Goldstone-mode contribution $1/[\mathcal{N}(1-G)]$ in Eq. (3.19) makes G smaller than unity, $1-G \cong \theta/\mathcal{N}$ at $\theta \ll 1$, which means that there is a gap in the correlation function $s_{\mathbf{q}}$. As a consequence, the magnetization m in Eq. (3.24) vanishes for $h \rightarrow 0$ for any finite \mathcal{N} . The same happens for low-dimensional systems $d \leq 2$, even in the bulk limit. In contrast, for three-dimensional bulk systems in zero field, G remains equal to 1 and the gap in the correlation function closes for $\theta \leq \theta_c = 1/W$. This is the

reason to call G the gap parameter. Below θ_c the spontaneous bulk magnetization is given by

$$m_b = \sqrt{1 - \theta/\theta_c} \quad (3.25)$$

The intrinsic magnetization of Eqs. (2.11) can with the help of Eqs. (3.18) and (3.19) be rewritten as

$$M = \sqrt{m^2 + \frac{\theta G}{\mathcal{N}(1-G)}} = \sqrt{1 - \theta G \tilde{P}_N(G)}, \quad (3.26)$$

where the last equality was inferred from the second of Eqs. (3.24). Note that m and M are related by Eq. (2.13) which is valid for all types of boundary conditions. Here $1 - G$ can be found from the first of Eqs. (3.24) and Eq. (2.13) as

$$1 - G \cong h/m \cong (h^*/2)[1 + \sqrt{1 + (2h/h^*)^2}], \quad (3.27)$$

where, for the moment, h^* is defined as $h^* = \theta/(\mathcal{N}M)$. With the help of these equations, the dependence $M = M(h, \theta)$ can be established perturbatively in different regions of the parameters. In particular, below θ_c for $\mathcal{N} \gg 1$ and $h \ll h^*$ one can use Eq. (3.23) with $1 - G \cong h^*[1 + (h/h^*)^2]$, which results in

$$M \cong m_b + \frac{\theta}{2m_b} \left\{ -W\Delta_N^{(\text{pbc})} + \frac{c\theta}{N^2 m_b} \left[1 + \left(\frac{h}{h^*} \right)^2 \right] \right\}, \quad h \ll h^*. \quad (3.28)$$

The last term in this expression cannot be obtained from the naive spin-wave theory. This term is very small, though. For $h^* \ll h$ one has $m \cong 1$ and $1 - G \cong h + h^*/2$. This yields the well-known singular \sqrt{h} spin-wave correction to the magnetization in three dimensions

$$M \cong m_b + \frac{\theta}{2m_b} \left\{ -W\Delta_N^{(\text{pbc})} + c_0\sqrt{h} \left(1 + \frac{h^*}{4h} \right) \right\}, \quad h^* \ll h \ll 1. \quad (3.29)$$

Note that a crossover between the different regimes occurs at $h \sim h^*$ for both the supermagnetization m , Eq. (2.13), and the intrinsic magnetization M , Eq. (3.26). At low temperatures in zero field M deviates from 1 according to the law

$$M \cong 1 - \theta W_N^{(\text{pbc})}/2, \quad (3.30)$$

where the coefficient in the linear- θ term is smaller than in the bulk [see Eq. (3.22)].

In spatial dimensions $d \leq 2$, $P(G)$ diverges for $G \rightarrow 1$, which rules out the long-range order in bulk systems. For any finite-size system, however, $M \rightarrow 1$ at low temperatures. In particular, in two dimensions one has $W_N^{(\text{pbc})} \cong 8\pi \ln N + \text{const}$, which results in

$$M \cong 1 - \theta(4\pi \ln N + \text{const}), \quad N \gg 1, \quad \theta \ll 1. \quad (3.31)$$

For the fields $h \gg 1, \theta$ one has, again, $m \cong 1$, $G \cong 1/(1+h) \ll 1$, $P(G) \cong 1$, and thus using the first of Eqs. (3.24) and the second equality in Eq. (3.26) one obtains

$$M \cong 1 - \frac{\theta}{2(1+h)}. \quad (3.32)$$

Here keeping 1 in the denominator improves the asymptotic behavior for moderately high values of h .

For the model with free boundary conditions, one cannot obtain a general analytical solution, and in the main range of temperatures and fields the problem has to be solved numerically. Analytical solutions exist, however, for high and low temperatures and for high fields. Before proceeding with the numerical solution of our problem, we will consider in the next section the most interesting analytical solution of the fbc model for $\theta \ll 1$.

4 Boundary effects at low temperature

At zero field the supermagnetization \mathbf{m} is zero, but in the limit of zero temperature all spins in the system become strongly correlated with each other: $s_{ij} \rightarrow 1$. For $\theta \ll 1$ one can search for the solution of Eqs. (2.5) and (2.6) in the form

$$s_{ij} \cong 1 - \delta s_{ij}, \quad G_i \cong G_i^{(0)} - \delta G_i, \quad (4.33)$$

where $G_i^{(0)}$ is the zero-temperature value of G_i whereas δs_{ij} and δG_i are small corrections. The zeroth order of Eq. (2.5) becomes

$$1 = G_i^{(0)} \sum_j \lambda_{ij} \quad (4.34)$$

which determines $G_i^{(0)}$. If the site i is not near the boundary so that all sites j are within the system, then the sum above and thus $G_i^{(0)}$ are equal to one. If i is near the boundary, some of the values of j run out of the system and are not counted, thus $G_i^{(0)}$ increases. For the sc lattice one has

$$\frac{1}{G_i^{(0)}} = 1 - \frac{1}{6}(\delta_{i_x,1} + \delta_{i_x,N} + \delta_{i_y,1} + \delta_{i_y,N} + \delta_{i_z,1} + \delta_{i_z,N}), \quad (4.35)$$

where $i \equiv \{i_x, i_y, i_z\}$. That is, $G_i^{(0)} = 6/5$ on the faces, $G_i^{(0)} = 3/2$ on the edges, and $G_i^{(0)} = 2$ at the corners.

In the first order in θ , Eqs. (2.6) and (2.7) become

$$\begin{aligned} \delta s_{ii} &= 0, \\ \sum_j \mathcal{D}_{ij}^{(0)} \delta s_{jl} &= -\theta \delta_{il} + \delta G_i / (G_i^{(0)})^2, \end{aligned} \quad (4.36)$$

where $\mathcal{D}_{ij}^{(0)}$ is the Dyson matrix defined in Eq. (2.7) taken at zero temperature. The solution of the linear problem above has the form

$$\begin{aligned} \delta G_i &= \theta (G_i^{(0)})^2 \sum_j \mathcal{D}_{ij}^{(0)} \mathcal{D}_{jj}^{-1(0)} \\ \delta s_{ij} &= \theta [\mathcal{D}_{ii}^{-1(0)} - \mathcal{D}_{ij}^{-1(0)}], \end{aligned} \quad (4.37)$$

where $\mathcal{D}_{ij}^{-1(0)}$ are the matrix elements of the inverse Dyson matrix $\mathcal{D}^{(0)}$.

The latter equations can be used to calculate different observables. In particular, the intrinsic magnetization M of Eq. (2.11) becomes

$$M \cong 1 - \frac{\theta}{2\mathcal{N}} \sum_{ij} \mathcal{D}_{ij}^{-1(0)} \left(\delta_{ij} - \frac{1}{\mathcal{N}} \right). \quad (4.38)$$

To evaluate the coefficient in the linear- θ term, it is convenient to expand $\mathcal{D}_{ij}^{-1(0)}$ over the set of eigenfunctions $F_{\mathbf{k}i}$ of the Dyson matrix $\mathcal{D}_{ij}^{(0)}$:

$$\mathcal{D}_{ij}^{-1(0)} = \sum_{\mathbf{k}} \frac{F_{\mathbf{k}i} F_{\mathbf{k}j}}{\mu_{\mathbf{k}}}, \quad (4.39)$$

where the eigenfunctions satisfy

$$\sum_i F_{\mathbf{k}i} \mathcal{D}_{ij}^{(0)} = \mu_{\mathbf{k}} F_{\mathbf{k}j}, \quad \sum_i F_{\mathbf{k}i} F_{\mathbf{k}'i} = \delta_{\mathbf{k}\mathbf{k}'}. \quad (4.40)$$

The latter can be found exactly since the matrix $\mathcal{D}_{ij}^{(0)}$ can be represented as a sum of three matrices:

$$\begin{aligned}\mathcal{D}_{ij}^{(0)} &= \mathcal{D}_{ij}^{x(0)} + \mathcal{D}_{ij}^{y(0)} + \mathcal{D}_{ij}^{z(0)}, \\ \mathcal{D}_{ij}^{x(0)} &= -(1/6)[\delta_{i_x, j_x-1} + \delta_{i_x, j_x+1} - \delta_{i_x, j_x}(2 - \delta_{j_x, 1} - \delta_{j_x, N})]\delta_{i_y, j_y}\delta_{i_z, j_z},\end{aligned}\quad (4.41)$$

etc., each of them acting as a discrete Laplace operator along the respective coordinate. Thus the variables separate

$$F_{\mathbf{k}i} = f_{i_x, k_x} \times f_{i_y, k_y} \times f_{i_z, k_z}, \quad \mu_{\mathbf{k}} = \tilde{\mu}_{k_x} + \tilde{\mu}_{k_y} + \tilde{\mu}_{k_z}, \quad (4.42)$$

and one obtains $\mu_{\mathbf{k}} = 1 - \lambda_{\mathbf{k}}$ and

$$f_{i_\alpha, k_\alpha} \propto \cos[(i_\alpha - 1/2)k_\alpha], \quad k_\alpha = \pi n_\alpha / N, \quad n_\alpha = 0, 1, \dots, N-1 \quad (4.43)$$

with $\alpha = z, y, z$.

Now, after substituting of Eq. (4.39) in Eq. (4.38), one obtains for $\theta \ll 1$

$$M \cong 1 - \frac{\theta}{2} W_N^{(\text{fbc})}, \quad W_N^{(\text{fbc})} = \frac{1}{\mathcal{N}} \sum_{\mathbf{k}}' \frac{1}{1 - \lambda_{\mathbf{k}}} \quad (4.44)$$

[cf. Eq. (3.30)]. It is interesting to note that $W_N^{(\text{fbc})}$ differs from $W_N^{(\text{pbc})}$ of Eq. (3.21) only by the definition of the discrete wave vectors, Eqs. (3.17) and (4.43), which results from different boundary conditions at the surfaces. In contrast to $W_N^{(\text{pbc})}$, the value of $W_N^{(\text{fbc})}$ exceeds the bulk value W , because the spins near the surface fluctuate stronger at finite temperatures. Moreover, it can be shown that in the isotropic semi-infinite system the magnetization profile is long ranged and decays as $1/z$, where z is the distance from the surface. Integrating this profile over the particle's volume gives $\Delta_N^{(\text{fbc})} = (W_N^{(\text{fbc})} - W)/W \propto \ln(N)/N$, i.e., the difference from the bulk value for the fbc system decreases slower than $\Delta_N^{(\text{pbc})}$ at large N . To obtain this result explicitly, one should bring $W_N^{(\text{fbc})}$ and $W_N^{(\text{pbc})}$ to the forms that are comparable with each other. To this end, we write $W_{2N}^{(\text{pbc})}$ in the form

$$W_{2N}^{(\text{pbc})} = \frac{1}{8\mathcal{N}} \sum_{\mathbf{k}}' \frac{1}{1 - \lambda_{\mathbf{k}}}, \quad k_\alpha = \frac{\pi n_\alpha}{N}, \quad n_\alpha = -N, \dots, N-1 \quad (4.45)$$

and complete the range of \mathbf{k} in Eq. (4.44) to that of the formula above. This results in the exact relation

$$\begin{aligned}W_N^{(\text{fbc})} &= W_{2N}^{(\text{pbc})} + \frac{9}{16\mathcal{N}} \sum_{k_x, k_y}' \frac{1}{(1 - \lambda_{\mathbf{k}}^{(2)})(2 - \lambda_{\mathbf{k}}^{(2)})} \\ &+ \frac{9}{\mathcal{N}} \sum_k' \frac{1}{(1 - \lambda_k^{(1)})(3 - \lambda_k^{(1)})(5 - \lambda_k^{(1)})} - \frac{7}{4\mathcal{N}},\end{aligned}\quad (4.46)$$

where $\lambda_{\mathbf{k}}^{(2)} \equiv (\cos k_x + \cos k_y)/2$, $\lambda_k^{(1)} \equiv \cos k$, and the additional terms arise because of the double counting on different faces, edges, and corners of the Brillouin zone as the completion is done. These terms can be loosely interpreted as contributions from faces, edges, and corners of the cube. One can see that in the large- N limit the face contributions are the most important ones and they behave as $\ln(N)/N$, whereas the edge contributions $\sim 1/N$ and the corner contributions $\sim 1/N^3$. The result for $\Delta_N^{(\text{fbc})}$ has the form

$$\Delta_N^{(\text{fbc})} \equiv \frac{W_N^{(\text{fbc})} - W}{W} \cong \frac{9 \ln(1.17N)}{2\pi N W}, \quad N \gg 1, \quad (4.47)$$

cf. Eq. (3.22). The next-to-log term in Eq. (4.47) is more difficult to obtain analytically; the best way is to fit the result of the direct numerical calculation of Eq. (4.44) (see Fig. 1).

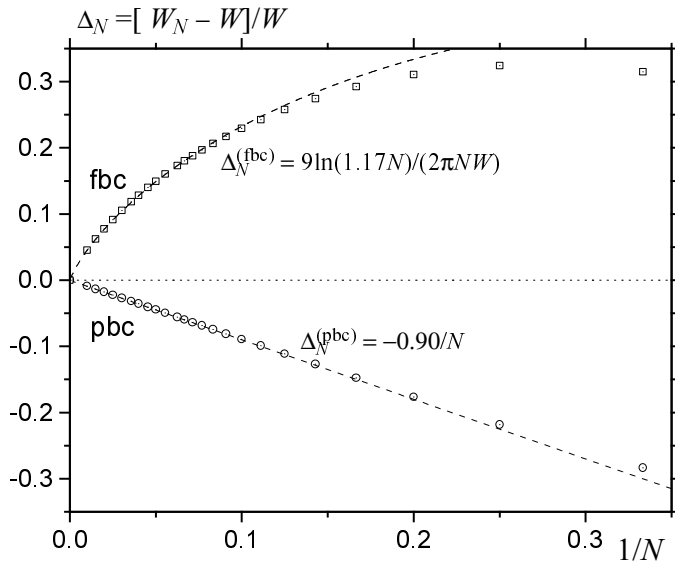


Fig. 1: Lattice sums W_N for the systems of the cubic form with free and periodic boundary conditions. $W = 1.51639$ is the bulk value for the sc lattice.

5 Numerical results

Here we present our numerical results for the temperature and field dependence of the intrinsic magnetization M and supermagnetization m for small magnetic systems with simple cubic lattice and cubic shape, subject to free and periodic boundary conditions (fbc and pbc). As was mentioned in Sec. 2, the numerical method for solving the $D \rightarrow \infty$ model consists in obtaining the correlation function s_{ij} and magnetization m_i from the linear equations (2.7), substituting them into the constraint equation (2.6), and solving the resulting nonlinear equation for the gap parameter G_i . On the first step we use a linear-equation solver based on the sparse-matrix storage appropriate for the Dyson matrix \mathcal{D} , which is defined by Eq. (2.7), in our case of nearest-neighbour interactions. The nonlinear problem is tackled using a nonlinear-equation solver of the Newton-Raphson kind. For the present geometry, symmetry arguments have been used to reduce the number of unknowns and thereby to increase the computing performance. The relevant subset of sites corresponding to different values of G_i is obtained by taking $1/8$ of the cube with a subsequent reduction by a factor of about $3!$ using permutations of the coordinates x , y , and z . This allows us to reduce the number of unknowns by a factor of about $8 \times 3! = 48$, this estimation becoming asymptotically exact for $\mathcal{N} \gg 1$. For the square lattice the reduction factor is about $4 \times 2! = 8$. All computations have been performed on a Pentium III/450 MHz of 128 MB RAM.

Fig. 2 shows the temperature dependence of the intrinsic magnetization M , Eq. (2.11), and local magnetizations M_i , Eq. (2.15), of the 14^3 cubic system with free and periodic boundary conditions in zero field. For periodic boundary conditions, M exceeds the bulk magnetization at all temperatures. In particular, at low temperatures this is in accord with the positive sign of the finite-size correction to the magnetization, Eqs. (3.29) and (3.22). The magnetization at the center of the cube with free boundary conditions is rather close to that for the model with pbc in the whole temperature range and converges with the latter at low temperatures. Local magnetizations at the center of the faces and edges and those at the corners decrease with temperature much faster than the magnetization at the center. This is also true for the intrinsic

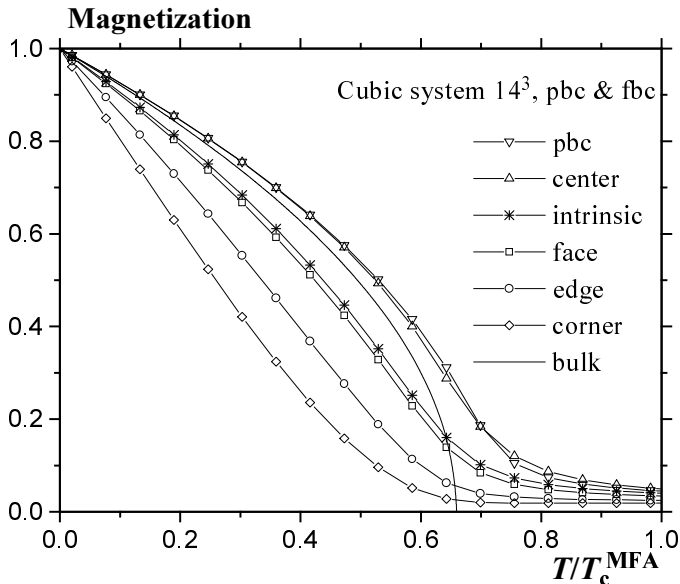


Fig. 2: Temperature dependence of the intrinsic magnetization M , Eq. (2.11), and local magnetizations M_i , Eq. (2.15), of the 14^3 cubic system with free and periodic boundary conditions in zero field.

magnetization M which is the average of the local magnetization M_i over the volume of the system: For the relatively small size 14^3 the contribution from the boundaries to the average properties are still substantial. One can see that, in the temperature range below the bulk critical temperature, M is smaller than the bulk magnetization. This means that the boundary effects suppressing M are stronger than the finite-size effects which lead to the increase of the latter. This is also seen from the low-temperature expression for M given in Eq. (4.44).

Magnetization profiles in the direction from the center of the cube to the center of a face are shown in Fig. 3 at different temperatures. One can see that perturbations due to the free boundaries extend deep into the system. This is a consequence of the Goldstone mode which renders the correlation length of an isotropic bulk magnet infinite below T_c . The latter effect is better seen from the magnified data at the low temperature (see the lower plot), where the MFA predicts, on the contrary, a fast approach to a constant magnetization when moving away from the surfaces [3]. MC simulations of the classical Heisenberg model [3, 4] also show long-range magnetization profiles. The difference of the local magnetizations in the center and at a surface point reaches a maximum in the vicinity of the bulk T_c and goes to zero at low and high temperatures.

Fig. 2 indicates that the critical indices for the magnetization at the faces, edges, and corners are higher than the bulk critical index $\beta = 1/2$ for the present $D = \infty$ model. The critical index at the face β_1 is the mostly studied surface critical index (see, for a review, Refs. [20, 21]). The exact solution of Bray and Moore [22] for the correlation functions at criticality in the $D = \infty$ model and application of the scaling arguments yield the value $\beta_1 = 1$ (see Table II in Ref. [20]). Exact values of the edge and corner magnetization indices, β_2 and β_3 , seem to be unknown for $D = \infty$. Cardy [23] used the first-order ε -expansion to obtain $\beta_2(\alpha)$ for the edge with an arbitrary angle α . For $\alpha = \pi/2$ and $D = \infty$ in three dimensions the result for the edge critical exponent reads $\beta_2 = 13/8 + O(\varepsilon^2) = 1.625 + O(\varepsilon^2)$.

To estimate the magnetization critical indices in our model we have performed a finite-size-scaling analysis (see, for a review, Ref. [24]) assuming the scaling form

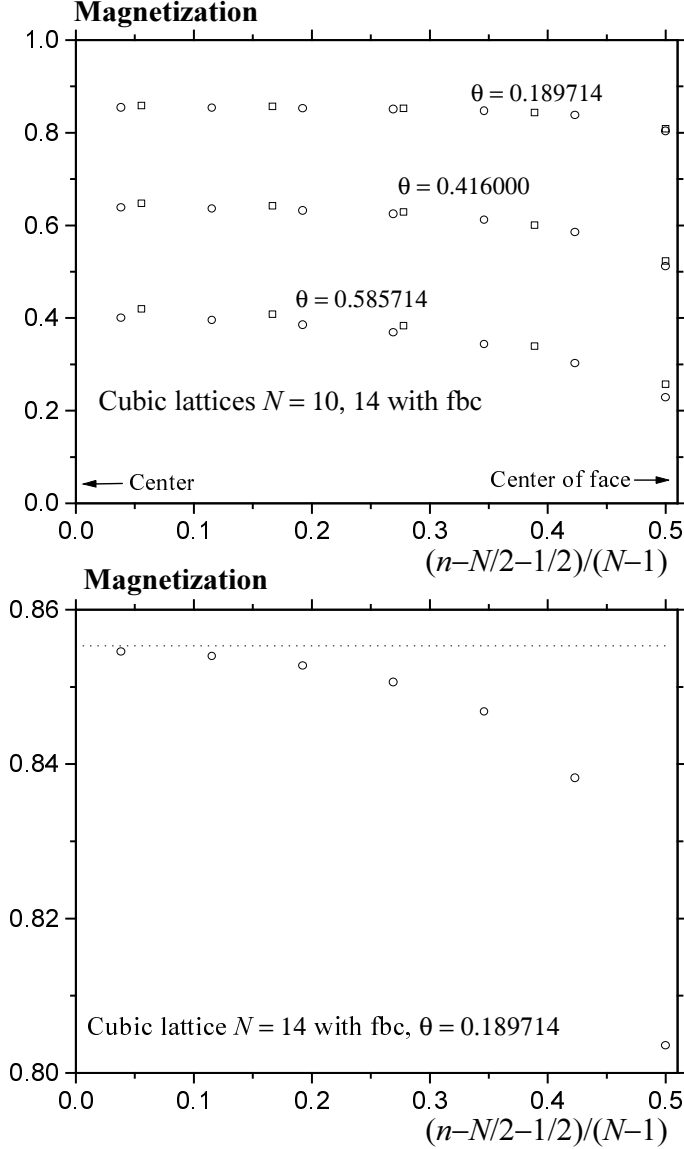


Fig. 3: Magnetization profiles in the direction from the center of the cube to the center of a face at different temperatures $\theta \equiv T/T_c^{\text{MFA}}$. The magnified lower plot shows the long-range character of the profile at low temperatures.

$M = N^{-\beta/\nu} F_M(\tau N^{1/\nu})$ and plotting in Fig. 4 the magnetization times $N^{\beta/\nu}$ vs $\tau N^{1/\nu}$. Here $\nu = 1$ is the critical index for the correlation length in the bulk and $\tau \equiv T/T_c - 1$, where $T_c = T_c^{\text{MFA}}/W$ is the bulk Curie temperature. Our results for the systems with $N = 10$ and $N = 14$ merge into single “master curves” for $\beta_1 = 0.86$, $\beta_2 = 1.33$, and $\beta_3 = 1.79$, which have been obtained by fitting $M \propto N^{-\beta/\nu}$ at $T = T_c$, i.e., $\theta = \theta_c = 1/W$. Note that our value 0.86 for the surface magnetization critical index β_1 is substantially lower than the value $\beta_1 = 1$ following from scaling arguments. This disagreement is probably due to corrections to scaling which could be pronounced for our insufficiently large linear sizes $N = 10$ and 14 . A more efficient way for obtaining an accurate value of β_1 is to perform a similar analysis for the semi-infinite model. The latter was considered analytically and numerically for $T \geq T_c$ and $H = 0$ in Ref. [14]. One should also mention the Monte Carlo simulations of the Ising model [25] which yield $\beta_1 = 0.80$, $\beta_2 = 1.28$, and $\beta_3 = 1.86$.

The field dependence of M and m at fixed temperature, as obtained from the

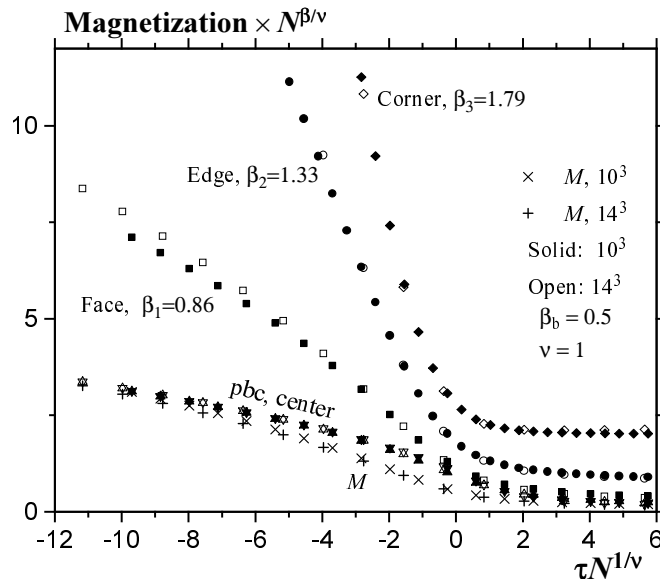


Fig. 4: Finite-size-scaling plot for the magnetization of cubic systems with linear size $N = 10$ and 14.

numerical solution of Eqs. (2.4) – (2.6), for cubic and square systems is shown in Fig. 5. Naturally the numerical results for m confirm Eq. (2.13) which describes both the effect of orientation of the system’s magnetization by the field and the increase of M in field. On the contrary, using the zero-field value of M in Eq. (2.13) leads to a poor result for m shown by the dashed curve for the 10^3 system in Fig. 5. Here we do see that there are two distinct field ranges separated by the characteristic field h^* , which were discussed at the end of Sec. 2. The results of Fig. 5 are in qualitative agreement with those of Fig. 1 in Ref. [18] showing the field dependence of $\chi = \partial m / \partial h$ obtained from phenomenological arguments. We should stress, however, that Eq. (2.13) which is *exact* in the $D = \infty$ model, has not yet been checked for systems with a finite number of spin components D and arbitrary size \mathcal{N} . The field dependence of the particle’s magnetization similar to that shown in Fig. 5 for the cubic system was experimentally obtained for ultrafine cobalt particles in recent Ref. [26], as well as in a number of previous experiments.

The curves for the square system in Fig. 5 illustrate the fact that in two dimensions thermal fluctuations are much stronger than in $3d$, which leads to lower values of both M and m at the same temperature. The bulk magnetization m_b in two dimensions vanishes at zero field and it thus goes below the intrinsic magnetization M in the low-field region.

6 Conclusion

In this paper, we have studied finite-size and boundary effects in small ferromagnetic systems with free boundaries within the $D = \infty$ classical vector model. This model, while sacrificing about 5% in the overall accuracy when used as a substitute for the Heisenberg model in three dimensions, is exactly solvable and describes relevant physical features related to the Goldstone modes, such as the absence of ordering in two dimensions for isotropic models, long-range magnetization profiles, etc. The $D = \infty$ model is clearly superior to the mean field approximation which ignores these important effects.

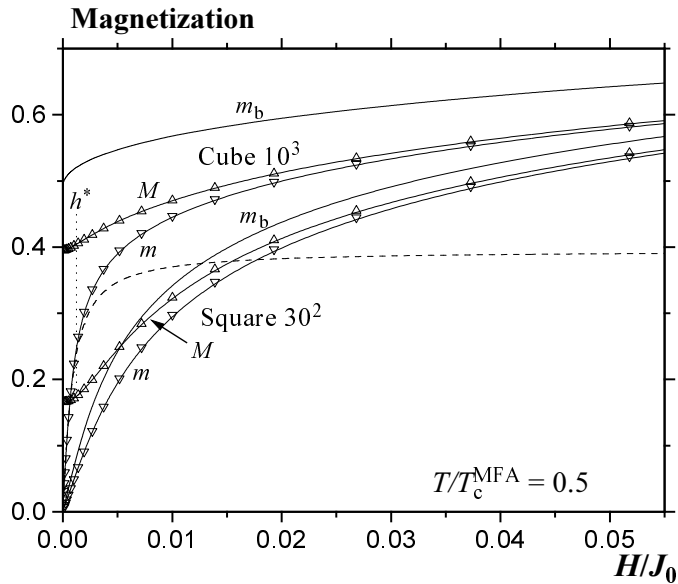


Fig. 5: Field dependence of the intrinsic magnetization M and supermagnetization m for hypercubic lattices with fbc in three and two dimensions. Dashed line is a plot of Eq. (2.13) in which $M(H, T)$ is replaced by its zero-field value. Bulk magnetization m_b in two and three dimensions is shown by solid lines.

An important result of our work is the exact relation of Eq. (2.13) between the intrinsic magnetization $M(H, T)$ and supermagnetization $m(H, T)$. It would be interesting to check whether this plausible relation holds for a more realistic Heisenberg model. In the latter case, it should be at least a good approximation.

Whereas the finite-size effects, which occur in a pure form in systems with periodic boundary conditions, lead to the increase of the magnetization with respect to the bulk value, boundary effects in systems with free boundaries work in the opposite direction. Since the magnetization reduction caused by the boundaries extends over the whole system (i.e., the magnetization profiles are long ranged), the boundary effect overweighs the finite-size effect by a large logarithmic contribution (see Fig. 1), and the resulting intrinsic magnetization M is lower than the bulk magnetization below the bulk critical temperature. The latter effect and the long-range magnetization profiles are illustrated in Figs. 2 and 3.

We have also attempted to estimate the surface magnetization critical indices for the faces, edges, and corners of the cube from the scaling analysis of the data for cubic systems with linear sizes $N = 10$ and $N = 14$. It seems that our values for all these indices are too low and the data for larger sizes are needed. The required computer resources, however, rapidly increase with the system's linear size N , since the theory operates with the correlation matrices of the size $N^3 \times N^3$.

Field dependences of the particle's supermagnetization m in Fig. 5 reflect both the *alignment* of the intrinsic magnetic moment M by the field and the *increase* of M in field. A combination of these two effects was observed in many experiments including the recent publication [26].

The present approach can be extended to magnetic systems of other shapes (spherical, cylindrical, etc.), more complicated lattice structures, and systems with a bulk and surface anisotropy. This will also allow us to compare with the results of the Monte Carlo simulations of a nanoparticle (of the maghemite type) studied in [4]. We are planning to study these issues in our future work.

Acknowledgements

D. A. Garanin is indebted to the Université de Versailles Saint Quentin and Laboratoire de Magnétisme et d'Optique for the warm hospitality extended to him during his stay in Versailles in July 1999 and January 2000. H. Kachkachi thanks Max-Planck-Institut für Physik komplexer Systeme Dresden for inviting him for a short stay in September 1999.

References

- [1] J.-L. Dormann, D. Fiorani, and E. Tronc, *Adv. Chem. Phys.* **98**, 283 (1997).
- [2] O. Eriksson, A. M. Boring, R. C. Albers, G. W. Fernando, and B. R. Cooper, *Phys. Rev. B* **45**, 2868 (1992).
- [3] V. Wildpaner, *Z. Phys. B* **270**, 215 (1974).
- [4] H. Kachkachi, A. Ezzir, M. Noguès, and E. Tronc, to appear in *Eur. Phys. J. B*.
- [5] H. E. Stanley, *Phys. Rev. Lett.* **20**, 589 (1968).
- [6] H. E. Stanley, *Physics Reports* **176**, 718 (1968).
- [7] T. N. Berlin and M. Kac, *Physics Reports* **86**, 821 (1952).
- [8] M. N. Barber and M. E. Fisher, *Ann. Phys. (N.Y.)* **77**, 1 (1973).
- [9] H. J. F. Knops, *J. Math. Phys.* **14**, 1918 (1973).
- [10] G. Costache, D. Mazilu, and D. Mihalache, *J. Phys. C* **9**, L501 (1976).
- [11] D. A. Garanin, *Z. Phys. B* **102**, 283 (1997).
- [12] D. A. Garanin, *J. Phys. A* **29**, 2349 (1996).
- [13] D. A. Garanin, *J. Phys. A* **29**, L257 (1996); **32**, 4323 (1999).
- [14] D. A. Garanin, *Phys. Rev. E* **58**, 254 (1998).
- [15] D. A. Garanin and V. S. Lutovinov, *Solid State Commun.* **50**, 219 (1984).
- [16] D. A. Garanin, *J. Stat. Phys.* **74**, 275 (1994).
- [17] D. A. Garanin, *Phys. Rev. B* **53**, 11593 (1996).
- [18] M. E. Fisher and V. Privman, *Phys. Rev. B* **32**, 447 (1985).
- [19] M. E. Fisher and V. Privman, *Commun. Math. Phys.* **103**, 527 (1986).
- [20] K. Binder, in *Phase Transitions and Critical Phenomena*, edited by C. Domb and J. L. Lebowitz (Academic Press, New York, 1983), Vol. 8.
- [21] H. W. Diehl, in *Phase Transitions and Critical Phenomena*, edited by C. Domb and J. L. Lebowitz (Academic Press, London, 1986), Vol. 10, pp. 75–267.
- [22] A. J. Bray and M. A. Moore, *Phys. Rev. Lett.* **38**, 735 (1977); *J. Phys. A* **10**, 1927 (1977).
- [23] J. L. Cardy, *J. Phys. A* **16**, 3617 (1983).

- [24] K. Binder, in *Computational Methods in Field Theory*, edited by H. Gausterer and C. B. Lang (Springer, Berlin, 1992).
- [25] M. Pleimling and W. Selke, **5**, 805 (1998).
- [26] M. Respaud, J. M. Broto, H. Rakoto, A. R. Fert, L. Thomas, B. Barbara, M. Verelst, E. Snoeck, P. Lecante, A. Mosset, J. Osuna, T. Ould Ely, C. Amiens, and B. Chaudret, *Phys. Rev. B* **57**, 2925 (1998).